

at lower temperatures and by the addition of excess alkyne to the solution, while formation of **6** is favored by longer reaction times, higher temperature, and no added alkyne. The paramagnetic cyclobutadienyl complex **7** is obtained only in very small amounts under any of these conditions. The structures of all three complexes have been confirmed by single-crystal X-ray analysis.<sup>6</sup>

Figure 1A is an ORTEP drawing of the structure of **5** (Ar = phenyl). The Mo–C1 and Mo–C4 distances are 1.946 (4) and 1.941 (4) Å, respectively, and are consistent with Mo=C bond orders of 2.7. The  $\pi$ -bonding in the metallacycle is not as localized in **5** as it is in **1** where there is a definite alternation in C–C bond lengths (C–C = 1.48, C=C = 1.39). In **5**, the C1–C2 and C3–C4 distances are 1.42 Å, and the C2–C3 bond is slightly longer, 1.44 Å. The structure of **5** is thus an example of the theoretically anticipated continuum between a metallacyclopentadiene and a metallacyclopentatriene (see ref 1).

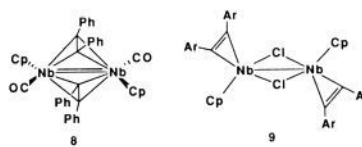
The MoC<sub>4</sub> ring is folded along the C1...C4 vector (dihedral angle = 117° versus 120° for **1**). According to our EHMO analysis, this folding results in a relief of anti-bonding interactions between Mo and C2, C3 despite the closer approach of C2, C3 (2.364 (4) and 2.350 (4) Å, respectively). In the planar structure,  $\pi$ -back bonding between Mo and the  $\pi_3^*$  LUMO of the C<sub>4</sub>R<sub>4</sub> ligand results in anti-bonding interactions between Mo and C2, C3 as a result of the nodal properties of the LUMO (see IV). When the ring is folded, one lobe of the d-orbital lies in the nodal plane of the C2, C3 p-orbitals, and the d–p overlap approaches zero (see V).



The structure of **6** (Ar = *p*-tolyl) is shown in Figure 1B. Assuming that the R<sub>4</sub>C<sub>4</sub><sup>2-</sup> ligand donates a total of eight electrons to the dimolybdenum frame, each Mo has a 16-electron count. However, if the cluster-counting rules<sup>8</sup> are invoked, each R–C unit is counted as a three-electron vertex, and each CpClMo group is considered to donate 6 + 6 – 12 = 0 electrons to cluster bonding, then the Mo<sub>2</sub>C<sub>4</sub> cluster core has six bonding electron pairs (S). Hence, S = N (number of vertices) and a biccapped tetrahedral geometry is predicted.<sup>8b</sup> The structure of **6** may indeed be considered to be a biccapped tetrahedron (the two terminal R–C groups each span a triangular M<sub>2</sub>C face).

Compound **6** differs from previously reported “fly-over” complexes<sup>9</sup> in that the two terminal carbons of the R<sub>4</sub>C<sub>4</sub> bridging ligand and the two Mo atoms are nearly coplanar and the R<sub>4</sub>C<sub>4</sub> plane is nearly perpendicular to the Mo–Mo vector. Some relevant distances are as follows: Mo–Mo' = 2.933 (1), Mo1–C14 = 2.065 (3), Mo1–C14' = 2.082 (3), Mo1–C6 = 2.240 (3), Mo1–C6' = 2.271 (3), C6–C14 = 1.478 (5), and C6–C6' = 1.504 (6) Å. The Mo–C14 bond lengths are just outside the range normally associated with Mo=C alkylidenes,<sup>7</sup> and the Mo–C6 distances are about 0.05 Å shorter than usual Mo–C single bonds.

The structure of **6** is even more astonishing when compared to that of the isoelectric complex [CpNb(CO)]<sub>2</sub>(Ph<sub>2</sub>C<sub>2</sub>)<sub>2</sub> (**8**). In compound **8**, the alkynes remain uncoupled, and the Nb atoms achieve an 18-electron count by forming a Nb=Nb double bond.<sup>10</sup>



In a similar vein (CpNbCl)<sub>2</sub>(R<sub>2</sub>C<sub>2</sub>)<sub>2</sub> (**9**), which has two electrons less than **6**, adopts an 18-electron count, chloro-bridged structure.<sup>11</sup> Further investigations of the factors which control the structures of M<sub>2</sub>(CR)<sub>4</sub> complexes are in progress.

**Acknowledgment.** We thank the donors of the Petroleum Research Fund, administered by the American Chemical Society, and the National Science Foundation (CHE-8619864) for support of this research. We also thank W. M. Butler and M.-S. Lah for the X-ray structure determinations.

**Supplementary Material Available:** Tables of crystallographic statistics, atomic coordinates, selected bond distances and angles and ORTEPs with complete numbering schemes for compounds **5**·CH<sub>2</sub>Cl<sub>2</sub>, **6**, and **7**·CH<sub>2</sub>Cl<sub>2</sub> (11 pages). Ordering information is given on any current masthead page.

(10) Nesmeyanov, A. N.; Gusev, A. I.; Pasynskii, A. A.; Anisimov, K. N.; Kolobova, N. E.; Struchkov, Yu. T. *J. Chem. Soc., Chem. Commun.* **1968**, 1365.

(11) Curtis, M. D.; Real, J. *Organometallics* **1985**, *4*, 940.

## Synthesis and Characterization of 12-Vertex Dinuclear Cobaltaborane Complexes Containing the Co<sub>2</sub>(CO)<sub>5</sub> Moiety and SEt<sub>2</sub> Cage Substituents

David M. Schubert, Carolyn B. Knobler, Patrick A. Wegner,<sup>1</sup> and M. Frederick Hawthorne\*

Department of Chemistry and Biochemistry  
The University of California, Los Angeles  
Los Angeles, California 90024

Received March 14, 1988

Although many parallels exist between metal carbonyl and boron hydride clusters, examples of larger boron hydride polyhedra that incorporate metal carbonyl cluster fragments are lacking. Furthermore, while a few dinuclear icosahedral metallaborane and metallacarborane clusters bearing cyclopentadiene ligands have been reported,<sup>2</sup> the synthesis of similar clusters possessing carbonyl groups have not been described. We report herein the synthesis of icosahedral dicobaltaborane carbonyl complexes of the type *closo*-B<sub>10</sub>H<sub>8</sub>(SEt<sub>2</sub>)<sub>2</sub>Co<sub>2</sub>(CO)<sub>5</sub>.

Reactions of the decaborane–Lewis base complex *arachno*-B<sub>10</sub>H<sub>12</sub>(SEt<sub>2</sub>)<sub>2</sub> with alkynes to give *closo*-1,2-C<sub>2</sub>B<sub>10</sub>H<sub>12</sub> or its C-substituted derivatives are well known.<sup>3</sup> Analogous insertions of transition-metal carbonyl cluster fragments into the decaborane cage to produce dinuclear icosahedral metallaboranes have not been previously exploited. We have recently found that reactions of *arachno*-B<sub>10</sub>H<sub>12</sub>(SEt<sub>2</sub>)<sub>2</sub> with Co<sub>2</sub>(CO)<sub>8</sub> or Co<sub>4</sub>(CO)<sub>12</sub> result in

(1) Department of Chemistry, California State University, Fullerton.

(2) (a) Sullivan, P. B.; Leyden, R. N.; Hawthorne, M. F. *J. Am. Chem. Soc.* **1975**, *97*, 455–456. (b) Leyden, R. N.; Sullivan, B. P.; Baker, R. T.; Hawthorne, M. F. *J. Am. Chem. Soc.* **1978**, *100*, 3758–3765. (c) Bowser, J. R.; Bonny, A.; Pipal, J. R.; Grimes, R. N. *J. Am. Chem. Soc.* **1979**, *101*, 6229–6236. (d) Evans, W. J.; Hawthorne, M. F. *J. Chem. Soc., Chem. Commun.* **1972**, 611–612. (e) Evans, W. J.; Dunks, G. B.; Hawthorne, M. F. *J. Am. Chem. Soc.* **1973**, *95*, 4565–4574. (f) Evans, W. J.; Hawthorne, M. F. *Inorg. Chem.* **1974**, *13*, 869–874. (g) Evans, W. J.; Hawthorne, M. F. *J. Am. Chem. Soc.* **1974**, *96*, 301–302. (h) Evans, W. J.; Jones, C. J.; Stibr, B.; Grey, R. A.; Hawthorne, M. F. *J. Am. Chem. Soc.* **1974**, *96*, 7405–7410.

(3) *Carboranes*; Grimes, R. N., Ed.; Academic Press: New York, 1970.

(6) Summary of crystallographic data (complete table in Supplementary Material). For **5**·CH<sub>2</sub>Cl<sub>2</sub> (Ar = phenyl) *a* = 10.039 (4) Å, *b* = 11.7609 (3) Å, *c* = 12.674 (8) Å,  $\alpha$  = 92.21 (4)°;  $\beta$  = 87.35 (4)°;  $\gamma$  = 104.05 (3)°, space group = *P* $\bar{1}$ , *Z* = 2, *R* = 0.038. For **6** (Ar = *p*-tolyl): *a* = 16.354 (2) Å, *b* = 10.436 (2) Å, *c* = 20.955 (7) Å,  $\beta$  = 103.19 (2)°, space group = *C*<sub>2</sub>/*C*, *Z* = 4, *R* = 0.025. For **7**·CH<sub>2</sub>Cl<sub>2</sub> (Ar = phenyl): *a* = 27.12 (4) Å, *b* = 11.42 (1), *c* = 19.32 (2) Å, orthorhombic, space group = *Pbca*, *Z* = 8, *R* = 0.062.

(7) Curtis, M. D.; Shiu, K.-B.; Butler, W. M. *J. Am. Chem. Soc.* **1986**, *108*, 1550.

(8) (a) Wade, K. *Transition-Metal Clusters*; Johnson, B. F. G., Ed.; Wiley: New York, 1980; pp 193–264. (b) Johnson, B. F. G.; Lewis, J. *Adv. Inorg. Chem. Radiochem.* **1981**, *24*, 225.

(9) (a) Knox, S. A.; Stansfield, R. F.; Stone, F. G. A.; Winter, M. J.; Woodward, P. *J. Chem. Soc., Dalton Trans.* **1982**, 173. (b) Dettlaf, G.; Weiss, E. *J. Organomet. Chem.* **1976**, *108*, 213. (c) Chisholm, M. H.; Hoffman, D. M.; Huffman, J. C. *J. Am. Chem. Soc.* **1984**, *106*, 6806.

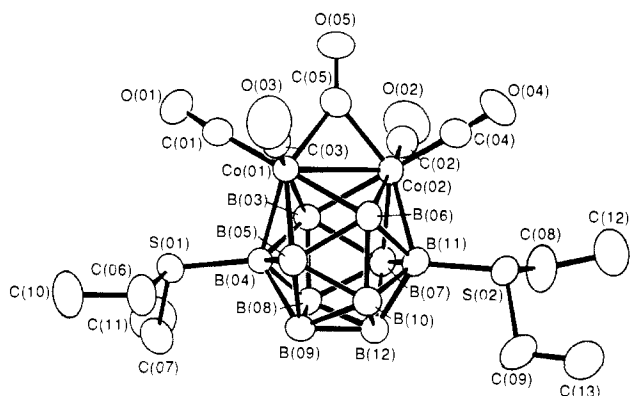


**Figure 1.** Structure of *closo*-1,1,2,2-(CO)<sub>4</sub>-1,2-μ-(CO)-4,11-(SEt<sub>2</sub>)<sub>2</sub>-1,2-Co<sub>2</sub>B<sub>10</sub>H<sub>8</sub>, **1**, with hydrogen atoms omitted for clarity. Interatomic distances [Å (esd)]: Co(O1)–Co(O2) = 2.490 (1); av S–B = 1.924 (6); av Co–C<sub>term</sub> = 1.769 (6); av C(O5)–Co = 1.894 (6); av C<sub>term</sub>–O<sub>term</sub> = 1.135 (7); C(O5)–O(O5) = 1.179 (6). Angles [deg (esd)]: Co(O1)–C(O5)–Co(O2) = 82.2 (2); av C<sub>term</sub>–Co–C<sub>term</sub> = 97.7 (3); av C(O5)–Co–C<sub>term</sub> = 92.7 (3).

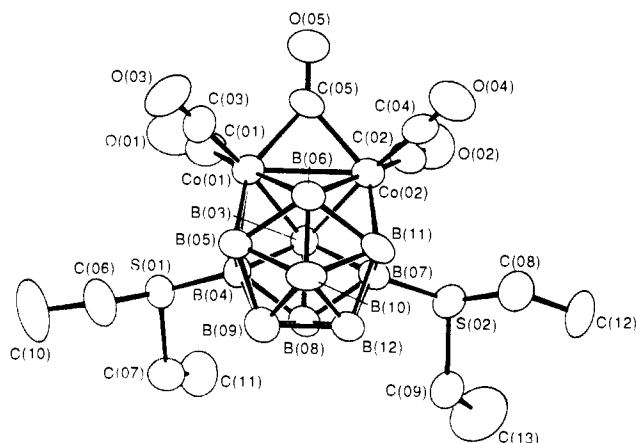
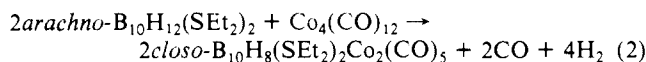
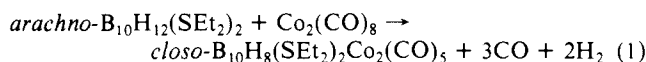


**Figure 2.** Structure of *closo*-1,1,2,2-(CO)<sub>4</sub>-1,2-μ-(CO)-4,7-(SEt<sub>2</sub>)<sub>2</sub>-1,2-Co<sub>2</sub>B<sub>10</sub>H<sub>8</sub>, **2**, with hydrogen atoms omitted for clarity. Interatomic distances [Å (esd)]: Co(O1)–Co(O2) = 2.488 (2); av S–B = 1.944 (11); av Co–C<sub>term</sub> = 1.77 (1); av C(O5)–Co = 1.90 (1); av C<sub>term</sub>–O<sub>term</sub> = 1.14 (1); C(O5)–O(O5) = 1.19 (1). Angles [deg (esd)]: Co(O1)–C(O5)–Co(O2) = 82.0 (4); av C<sub>term</sub>–Co–C<sub>term</sub> = 97.0 (5); av C(O5)–Co–C<sub>term</sub> = 93.8 (4).

the formation of dinuclear cobaltaborane complexes, apparently as in eq 1 and 2.<sup>4</sup> The major product of these reactions consists



of two isomers which can be separated by column chromatography to give nearly equal quantities of air-stable, crystalline complexes in combined purified yields of 43% (eq 1) and 48% (eq 2). These isomers have been characterized as *closo*-1,1,2,2-(CO)<sub>4</sub>-1,2-μ-CO-4,11-(SEt<sub>2</sub>)<sub>2</sub>-1,2-Co<sub>2</sub>B<sub>10</sub>H<sub>8</sub> (**1**)<sup>5</sup> and *closo*-1,1,2,2-(CO)<sub>4</sub>-1,2-μ-CO-4,7-(SEt<sub>2</sub>)<sub>2</sub>-1,2-Co<sub>2</sub>B<sub>10</sub>H<sub>8</sub> (**2**).<sup>6</sup>

Structures of **1** and **2**, shown in Figures 1 and 2, were determined by single-crystal X-ray diffraction studies.<sup>7</sup> Each cluster

contains two cobalt centers that participate in a Co<sub>2</sub>(CO)<sub>5</sub> moiety as encountered in Co<sub>4</sub>(CO)<sub>12</sub> (**3**)<sup>8</sup> and [HC<sub>3</sub>(CO)<sub>10</sub>]<sup>−</sup> (**4**).<sup>9</sup> Also, diethyl sulfide molecules formally replace terminal hydride ligands on two boron atoms in each complex. Complex **1** possesses a noncrystallographic local twofold rotation axis, and **2** contains a noncrystallographic local mirror plane. Corresponding distances and angles are very similar in **1** and **2**. The Co–Co interatomic distances average 2.489 (2) Å (cf. 2.483 Å in **3** and 2.474 Å in **4**).<sup>8,9</sup> The geometry about each sulfur atom is pyramidal. Average B–B and Co–B bond lengths are 1.78 and 2.17 Å, respectively. These complexes belong to a family of formally zwitterionic B-substituted boron cage compounds bearing dialkylsulfonium groups.<sup>10</sup>

Mass spectra show parent ion envelopes accompanied by four envelopes corresponding to successive loss of CO from the parent ions. Intense peaks also occur at 90 *m/e* corresponding to the [SEt<sub>2</sub>]<sup>+</sup> ion. The 160.5 MHz <sup>11</sup>B{<sup>1</sup>H} NMR spectrum of **1** exhibits four resonances in 2:4:2:2 area ratios, while the spectrum of **2** shows six resonances in 1:2:2:1:2:2 ratios, consistent with the solid-state structures. Both isomers exhibit complex room temperature <sup>1</sup>H NMR spectra indicative of hindered internal rotation about boron–sulfur bonds. The 23 °C 500.1 MHz <sup>1</sup>H NMR spectrum of each complex shows two triplet methyl and four six-line (1:2:3:3:2:1) multiplet methylene resonances, the multiplets being produced by overlap of the expected four doublet of quartet resonances. Assignments of coupled nuclei were made by using the COSY technique, and spectra could be computer simulated.

Dynamic behavior of **1** and **2** was studied by VT <sup>1</sup>H NMR spectroscopy. Upon warming toluene solutions of either complex above room temperature, both methyl and methylene resonances broaden and coalesce. At 110 °C each isomer exhibits a single

(4) **1** and **2**: diethyl sulfide (10 mL, 0.09 mol) was added to 5.0 g of *nido*-B<sub>10</sub>H<sub>14</sub> (0.041 mol) in 200 mL of toluene. The solution was stirred for 3 h at 40 °C and then for 2 h at 65 °C. Dicobalt octacarbonyl (14.0 g, 0.041 mol) in 400 mL of toluene was added, and the mixture was stirred at 85 °C for 16 h and then at reflux for 3 h. The solution was filtered, and remaining solid was extracted with toluene. Solvent was removed in vacuo, and the crude product was purified by column chromatography on alumina. Two yellow bands were eluted with toluene, and products were recrystallized from methylene chloride/pentane. The first band, **1**, produced orange needles (5.02 g, 22%, dec >198 °C) and the second band, **2**, orange plates (4.82 g, 21% yield, mp 178–180 °C, dec). Similarly, 425 mg of B<sub>10</sub>H<sub>14</sub> (3.5 mmol), 0.75 mL of SEt<sub>2</sub> (7.1 mmol), and 1.00 g of Co<sub>4</sub>(CO)<sub>12</sub> (1.7 mmol) resulted in 0.47 g (24%) of **1** and 0.46 g (24%) of **2**.

(5) **1**: 160.5 MHz <sup>11</sup>B NMR (C<sub>7</sub>H<sub>8</sub>, ref BF<sub>3</sub>·OEt<sub>2</sub>, 23 °C, ppm) δ −12.8 (d, 2), 2.3 (d, 2), 9.8 (m, 4), 11.9 (d, 2); 500.1 MHz <sup>1</sup>H NMR (C<sub>7</sub>D<sub>8</sub>, 23 °C, ppm) (a) δ 0.64 (t, CH<sub>3</sub>), (b) 0.88 (t, CH<sub>3</sub>), (c) 2.07 (d of q, CH<sub>2</sub>), (d) 2.21 (d of q, CH<sub>2</sub>), (e) 2.67 (d of q, CH<sub>2</sub>), (f) 2.81 (d of q, CH<sub>2</sub>) [<sup>3</sup>J(H<sub>a</sub>–H<sub>d</sub>) = <sup>3</sup>J(H<sub>b</sub>–H<sub>e</sub>) = 7.4 Hz, <sup>2</sup>J(H<sub>c</sub>–H<sub>f</sub>) = 13.5 Hz]; 125.8 MHz <sup>13</sup>C{<sup>1</sup>H} NMR (CD<sub>2</sub>Cl<sub>2</sub>, 23 °C, ppm) δ 12.44 (CH<sub>3</sub>), 12.56 (CH<sub>3</sub>), 35.24 (CH<sub>2</sub>), 36.30 (CH<sub>2</sub>); IR (Nujol, cm<sup>−1</sup>) 2497 s, 2062 s, 2034 s, 1998 s, 1823 s; MS (*m/e*) (rel intensity) 556 (2, <sup>12</sup>C<sub>13</sub><sup>1</sup>H<sub>28</sub><sup>16</sup>O<sub>5</sub><sup>11</sup>B<sub>10</sub><sup>32</sup>S<sub>2</sub><sup>59</sup>Co<sub>2</sub><sup>+</sup>), 75 (100, <sup>12</sup>C<sub>13</sub><sup>1</sup>H<sub>7</sub><sup>32</sup>S<sup>+</sup>), 90 (96, <sup>12</sup>C<sub>13</sub><sup>1</sup>H<sub>10</sub><sup>32</sup>S<sup>+</sup>); UV–vis (CH<sub>2</sub>Cl<sub>2</sub>) λ<sub>max</sub> [ε (M<sup>−1</sup> cm<sup>−1</sup>)] 230 (2690), 259 (2000), 424 nm (160). Anal. Calcd for C<sub>13</sub>H<sub>28</sub>O<sub>5</sub>B<sub>10</sub>S<sub>2</sub>Co<sub>2</sub>: C, 28.16; H, 5.09; B, 19.50; S, 11.57; Co, 21.26. Found: C, 27.37; H, 5.21; B, 20.22; S, 11.77; Co, 19.54.

(6) **2**: 160.5 MHz <sup>11</sup>B NMR (C<sub>7</sub>H<sub>8</sub>, ref BF<sub>3</sub>·OEt<sub>2</sub>, 23 °C, ppm) δ −17.3 (d, 2), −8.5 (d, 2), 3.3 (d, 1), 7.1 (s, 2), 10.8 (d, 2), 13.5 (d, 2); 500.1 MHz <sup>1</sup>H NMR (C<sub>7</sub>D<sub>8</sub>, 23 °C, ppm) (a) δ 0.75 (t, CH<sub>3</sub>), (b) 0.88 (t, CH<sub>3</sub>), (c) 2.18 (d of q, CH<sub>2</sub>), (d) 2.30 (d of q, CH<sub>2</sub>), (e) 2.71 (d of q, CH<sub>2</sub>), (f) 2.86 (d of q, CH<sub>2</sub>) [<sup>3</sup>J(H<sub>a</sub>–H<sub>d</sub>) = <sup>3</sup>J(H<sub>b</sub>–H<sub>e</sub>) = 7.5 Hz, <sup>2</sup>J(H<sub>c</sub>–H<sub>f</sub>) = <sup>2</sup>J(H<sub>d</sub>–H<sub>f</sub>) = 12.58 Hz]; 125.8 MHz <sup>13</sup>C{<sup>1</sup>H} NMR (CD<sub>2</sub>Cl<sub>2</sub>, 23 °C, ppm) δ 12.74 (CH<sub>3</sub>), 12.94 (CH<sub>3</sub>), 35.53 (CH<sub>2</sub>), 36.44 (CH<sub>2</sub>); IR (Nujol, cm<sup>−1</sup>) 2499 s, 2060 s, 2021 s, 1825 s; MS (*m/e*) (rel intensity) 556 (2, <sup>12</sup>C<sub>13</sub><sup>1</sup>H<sub>28</sub><sup>16</sup>O<sub>5</sub><sup>11</sup>B<sub>10</sub><sup>32</sup>S<sub>2</sub><sup>59</sup>Co<sub>2</sub><sup>+</sup>), 75 (100, <sup>12</sup>C<sub>13</sub><sup>1</sup>H<sub>7</sub><sup>32</sup>S<sup>+</sup>), 90 (97, <sup>12</sup>C<sub>13</sub><sup>1</sup>H<sub>10</sub><sup>32</sup>S<sup>+</sup>); UV–vis (CH<sub>2</sub>Cl<sub>2</sub>) λ<sub>max</sub> [ε (M<sup>−1</sup> cm<sup>−1</sup>)] 229 (2690), 253 (1900), 424 nm (145). Anal. Calcd for C<sub>13</sub>H<sub>28</sub>O<sub>5</sub>B<sub>10</sub>S<sub>2</sub>Co<sub>2</sub>: C, 28.16; H, 5.09; B, 19.50; S, 11.57; Co, 21.26. Found: C, 28.23; H, 5.30; B, 20.38; S, 11.74; Co, 19.99.

(7) **1**: monoclinic, *P*2<sub>1</sub>/*c*, *a* = 17.3779 (10) Å, *b* = 8.8330 (5) Å, *c* = 17.9275 (9) Å, β = 112.080 (1)°, *Z* = 4. **2**: monoclinic, *C*2/*c*, *a* = 17.455 (1) Å, *b* = 12.395 (1) Å, *c* = 24.251 (2) Å, β = 105.449 (2)°, *Z* = 8. Structures were solved by using MULTAN80 for **1** and heavy atom methods for **2**. Non-hydrogen atoms were refined anisotropically by full-matrix least-squares methods. Refinement for **1** using 2664 reflections (*I* > 3σ(*I*), 3998 unique reflections) converged at *R* = 3.9% (*R*<sub>w</sub> = 4.9, GOF = 1.50) and for **2** using 2420 reflections (*I* > 3σ(*I*), 3984 unique reflections) converged at *R* = 6.5% (*R*<sub>w</sub> = 7.9, GOF = 2.13).

(8) Carre, F. H.; Cotton, F. A.; Frenz, B. A. *Inorg. Chem.* **1976**, *15*, 380–387.

(9) Adams, H.-N.; Fachinetti, G.; Strahle, J. *Angew. Chem., Int. Ed. Engl.* **1980**, *19*, 404–405.

(10) (a) Plešek, J.; Janousek, Z.; Hermanek, S. *Collec. Czech. Chem. Commun.* **1978**, *43*, 1332–1338. (b) Young, D. C.; Howe, D. V.; Hawthorne, M. F. *J. Am. Chem. Soc.* **1969**, *91*, 859–862. (c) Plešek, J.; Janousek, Z.; Hermanek, S. *Collec. Czech. Chem. Commun.* **1978**, *43*, 2862–2868. (d) Hawthorne, M. F.; Warren, L. F.; Callahan, K. P.; Travers, N. F. *J. Am. Chem. Soc.* **1971**, *93*, 2407–2412.

sharp triplet methyl resonance indicative of rapid ethyl group exchange on the NMR time scale. Coalescence temperatures for internal rotation were 85 °C for **1** and 78 °C for **2**. Activation energies for this process were 17.8 kcal·mol<sup>-1</sup> for each isomer.<sup>11</sup> A similar hindered rotation has been noted for [nido-9-SMe<sub>2</sub>-7,8-C<sub>2</sub>B<sub>9</sub>H<sub>11</sub>]<sup>-</sup>.<sup>10c</sup>

Formation of isomers in a 1:1 statistical ratio suggests a mechanism wherein diethyl sulfide is initially lost from B<sub>10</sub>H<sub>12</sub>(SEt<sub>2</sub>)<sub>2</sub> and recaptured upon formation of **1** and **2**. This process may be related to the acid-catalyzed nucleophilic substitution reaction as it occurs in the formation of [M-(C<sub>2</sub>B<sub>9</sub>H<sub>11</sub>)(C<sub>2</sub>B<sub>9</sub>H<sub>10</sub>SEt<sub>2</sub>)] (M = Fe, Co) upon reaction of diethyl sulfide with protonated [M(C<sub>2</sub>B<sub>9</sub>H<sub>11</sub>)<sub>2</sub>]<sup>-</sup> (M = Fe, Co).<sup>10d</sup>

**Acknowledgment.** This work was supported by the National Science Foundation (Grant CHE-84-01433). We thank Julie Maurer for the COSY spectra and Andrea Owyung for the illustrations.

**Supplementary Material Available:** Tables of positional and thermal parameters and interatomic distances and angles for **1** and **2** (16 pages). Ordering information is given on any current masthead page.

(11) Free energies of activation ( $\Delta G^\ddagger$ ) were obtained at coalescence temperatures by means of the Eyring equation and the expression  $k = \pi\Delta\nu/2^{1/2}$ .

### Use of a Polymeric Counterion To Induce Bilayer Formation from a Single-Chain Surfactant<sup>1</sup>

Masa-aki Wakita,<sup>2a</sup> Katherine A. Edwards,<sup>2b</sup> and Steven L. Regen\*

Department of Chemistry and Zettlemoyer Center  
for Surface Studies, Lehigh University  
Bethlehem, Pennsylvania 18015

David Turner and Sol M. Gruner

Department of Physics, Joseph Henry Laboratories  
Princeton University, Princeton, New Jersey 08544

Received March 7, 1988

Revised Manuscript Received May 20, 1988

In this paper we show that cetyltrimethylammonium bromide (CTAB), a common micelle-forming surfactant, is converted into a bilayer-forming polyelectrolyte when the bromide ion is replaced by poly(acrylate). This finding demonstrates the feasibility of using a polymeric counterion to control micellar/lamellar phase formation from a *single-chain surfactant* and establishes a new and unique class of surfactant vesicles.<sup>3</sup>

Although single-chain surfactants typically form micellar aggregates in aqueous media,<sup>4</sup> we sought to investigate whether single-chain surfactants paired with polymeric counterions might produce a lamellar phase. In particular, we reasoned that organic counterions, held in close mutual proximity along a polymer backbone, could promote (i) tight ion pairing, (ii) reduced electrostatic repulsion between (and hydration of) the head groups, and (iii) enhanced lateral interaction among the surfactant chains.<sup>5</sup>

(1) Supported by the National Science Foundation (CHE 87-00833) and Kurita Water Industries, Ltd. (Tokyo, Japan).

(2) (a) On leave from Kurita Water Industries, Ltd. (b) NSF-REU undergraduate.

(3) Evans, D. F.; Ninham, B. W. *J. Phys. Chem.* **1986**, *90*, 226. Brady, J. E.; Evans, D. F.; Kachar, B.; Ninham, B. W. *J. Am. Chem. Soc.* **1984**, *106*, 4279.

(4) For examples of rare exceptions, see: Hicks, M.; Gebicki, J. M. *Chem. Phys. Lipids* **1977**, *20*, 243. Hargreaves, W. R.; Deamer, D. W. *Biochemistry* **1978**, *17*, 3759. Jain, M. K.; van Echteld, J. A.; Ramirez, F.; deGier, J.; De Haas, G. H.; van Deenen, L. L. M. *Nature (London)* **1980**, *284*, 486. Kunitake, T.; Okahata, Y.; Shimomura, M.; Yasunami, S.; Takarabe, K. *J. Am. Chem. Soc.* **1981**, *103*, 5401. Tilcock, C. P. S.; Cullis, P. R.; Hope, M. J.; Gruner, S. M. *Biochemistry* **1986**, *25*, 816.

(5) Fukuda, H.; Diem, T.; Stefely, J.; Kezdy, F. J.; Regen, S. L. *J. Am. Chem. Soc.* **1986**, *108*, 2321.

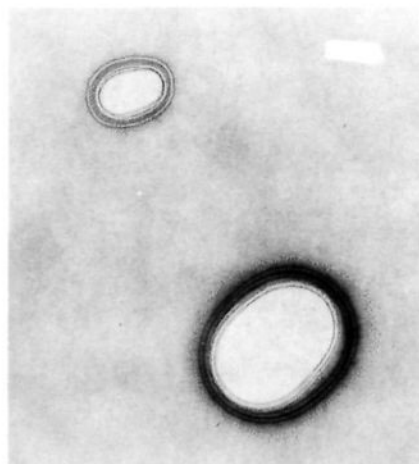
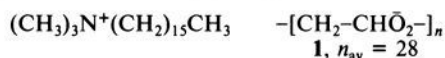


Figure 1. Transmission electron micrograph of an unstained dispersion of **1**; bar represents 1000 Å.

In terms of the packing of the molecules, we hypothesized that a reduction in the effective interfacial headgroup area might promote the formation of a lamellar phase. Further, given the low cost and ready availability of a wide variety of single-chain surfactants, together with the potential utility of surfactant vesicles for device applications,<sup>6</sup> such a finding would be of both theoretical and practical interest. In this report, we confirm this hypothesis by showing that bilayer vesicles are produced from common and inexpensive poly(acrylic acid) and CTAB precursors.

CTAB was converted into its hydroxide form via ion exchange (Amberlite IRA-400 (OH), Aldrich) and then combined with a stoichiometric quantity of poly(acrylic acid) (MW 2000, Aldrich) in methanol. Subsequent removal of solvent, and lyophilization from *tert*-butyl alcohol, afforded a 99% yield of poly(cetyltrimethylammonium acrylate) [**1**] as a white powder; analysis by IR (thin film on NaCl plates, deposited from a CHCl<sub>3</sub> solution) confirmed the complete disappearance of the carboxylic acid (1680 cm<sup>-1</sup>) and the appearance of ammonium carboxylate groups (1570, 1400 cm<sup>-1</sup>); thin layer chromatography [silica, CHCl<sub>3</sub>/CH<sub>3</sub>OH, 8/2 (v/v)] showed a single spot at the origin and the complete disappearance of CTAB (*R<sub>f</sub>* 0.45).



Rapid injection of 35  $\mu\text{L}$  of a 0.124 M ethanolic solution of **1** into 1.5 mL of water produced a translucent dispersion.<sup>7</sup> Dynamic light scattering (Nicom 200, 632.8 nm, 90° scattering angle) indicated particles having diameters ranging between 800 and 3500 Å; examination by transmission electron microscopy (TEM) as *unstained* samples (Philips 400) revealed particles of similar size, comprised of well-defined concentric membranes (Figure 1).<sup>8</sup> The apparent thickness of these membranes (dark rings) was  $38 \pm 5$  Å, which is consistent with bilayer thicknesses found in other vesicles or liposomes.<sup>9</sup> Further examination of these particles using a through-focal series of micrographs confirmed that these images are due to a mass thickness contrast and are not derived from Fresnel fringe formation.

Passage of the dispersion through a Sephadex G-50 column afforded a 48% recovery in the void volume (nitrogen analysis).<sup>5</sup> In some preparations, a small amount of polymeric surfactant was detected beyond the void volume. Rechromatography of the vesicle fraction through a fresh Sephadex G-50 column afforded an 80%

(6) Fendler, J. H. *Chem. Rev.* **1987**, *87*, 877. Fendler, J. H. *Membrane Mimetic Chemistry*; Wiley-Interscience: New York, 1982.

(7) Batzri, S.; Korn, E. D. *Biochim. Biophys. Acta* **1973**, *298*, 1015.

(8) TEM micrographs of a similar sample, prepared by conventional negative staining procedures (2% uranyl acetate),<sup>5</sup> showed only closed spheres; discrete membrane walls were not detected.

(9) Bangham, A. D.; Hill, M. W.; Miller, N. G. A. In *Methods in Membrane Biology*; Korn, E. D., Ed.; Plenum: New York, 1974; Vol 1, p 1.